
Thermal Analysis for an Ultra High Temperature Gas-Cooled Reactor with Pebble Type Fuels

Motoo Fumizawa, Naoya Uchiyama, Takahiro Nakayama

Department of Mechanical Engineering, Shonan Institute of Technology, Fujisawa, Kanagawa, Japan

Email Address:

fumizawa@mech.shonan-it.ac.jp (M. Fumizawa), psn-man.lv.030@softbank.ne.jp (N. Uchiyama), 2991taka@gmail.com (T. Nakayama)

To cite this article:

Motoo Fumizawa, Naoya Uchiyama, Takahiro Nakayama. Thermal Analysis for an Ultra High Temperature Gas-Cooled Reactor with Pebble Type Fuels. *International Journal of Energy and Power Engineering*. Vol. 4, No. 4, 2015, pp. 189-196. doi: 10.11648/j.ijepe.20150404.11

Abstract: This study presents a predictive thermal-hydraulic analysis with packed spheres in a nuclear gas-cooled reactor core. The predictive analysis considering the effects of high power density and the some porosity value were applied as a design condition for an Ultra High Temperature Reactor (UHTR). The thermal-hydraulic computer code was developed and identified as PEBTEMP. The highest outlet coolant temperature of 1316 °C was achieved in the case of an UHTREX at LASL, which was a small scale UHTR using hollow-rod as a fuel element. In the present study, the fuel was changed to a pebble type, a porous media. Several calculation based on HTGR-GT300 through GT600 were 4.8 w/cm³ through 9.6 w/cm³, respectively. As a result, the relation between the fuel temperature and the power density was obtained under the different system pressure and coolant outlet temperature. Finally, available design conditions are selected.

Keywords: Thermal Hydraulics, Ultra High Temperature Reactor (UHTR), Pressure Drop, Porosity and Pebble Type Fuel

1. Introduction

Very high temperature gas-cooled reactor project is energetically developing the design study to establish 1,000 °C as a coolant outlet temperature and to realize the hydrogen production [1-2], where GIF is the Generation IV International Forum. For a long time, a fundamental design study has been carried out in the field of the high temperature gas-cooled reactor i.e. HTGR [3-8], which showed that a coolant outlet temperature was around 900 °C. The interest of HTGR is increasing in many countries as a promising energy future option. There are currently two research reactors of THGR type that are being operated in Japan and China. The inherent safety of HTGR is due to the large heat capacity and negative temperature reactivity coefficient. The high temperature heat supply can achieve more effective utilization of nuclear energy. For example, high temperature heat supply can provide for hydrogen production, which is expected as an alternative energy source for oil. Also, outstanding thermal efficiency will be achieved at about 900 °C with a Brayton-cycle gas turbine plant.

However, the highest outlet coolant temperature of 1316 °C had been achieved by UHTREX as shown in Figure 1, in Los Alamos Scientific Laboratory at the end of 1960's [3-4]. It was a small scale Ultra High Temperature Nuclear Reactor

(UHTR). The coolant outlet temperature would be higher than 1000 °C in the UHTR. The UHTREX adopted the hollow rod type fuel; the highest fuel temperature was 1,582 °C, which indicated that the value was over the current design limit. According to the handy calculation, it was derived that the pebble type fuel was superior to the hollow type in the field of fuel surface heat transfer condition [9]. In the present study, the fuels have changed to the pebble type so called the porous media. In order to compare the present pebble bed reactor and UHTREX, a calculation based on HTGR-GT300 was carried out in the similar conditions with UHTREX i.e. the inlet coolant temperature of 871 °C, system pressure of 3.45 MPa and power density of 1.3 w/cm³. The main advantage of the pebble bed reactor (PBR) is that high outlet coolant temperature can be achieved due to its large cooling surface and high heat transfer coefficient that have the possibility to get high thermal efficiency. Besides, the fuel loading and discharging procedures are simplified; the PBR system makes it possible that the frequent load and discharge are easier than the other reactor system loaded block type fuel without reactor shutdown. This report presents thermal-hydraulic calculated results for a concept design PBR system of 300MWth of the modular HTGR-GT300 with the pebble types of fuel element

as shown in Figure 2. A calculation for comparison with UHTREX have been carried out and presented as well.

2. Reactor Description

2.1. Concept of Modular HTGR-GT300, GT600 and GT600

A concept of pebble-bed type HTGR are shown in Figures 2 and 3 with the main nuclear and thermal-hydraulic specifications presented in Table 1. In the case that the thermal power is 300MW (GT-300), the average power density changes to 4.8 MW/m³. The coolant gas enters from the outer shell of the primary coolant coaxial tube to the pressure vessel at temperature of 550°C and pressure of 6 MPa, follows the peripheral region of side reflectors up to the top and goes downward through the reactor active core. The outlet coolant goes out through the inner shell of primary coolant tube at temperature of 900°C. The cylindrical core is formed by the blocks of graphite reflector with the height of 9.4m and the diameter of 2.91m. There exist holes in the reflector that some of them used for control rod channels and the others used for boron ball insertion in case of an accident. In the case that the thermal powers are 450MW (GT450) and 600MW (GT600), the average power densities change to 7.2 MW/m³ and 9.6 MW/m³, respectively.

2.2. Fuel Element

The two types of pebble fuel elements, consisting of fuel and moderator, are shown in Figure 4. One is a solid type where radius of inner graphite $r_{co}=0$, and the other is a shell type fuel element. The fuel compacts are a mixture of coated particles [9].

3. Thermhydraulic Analysis

3.1. PEPTEMP Code

A one-dimensional thermal-hydraulic computer code was developed that was named PEPTEMP [5] as shown in Figure 5. The code solves for the temperature of fuel element, coolant gas and core pressure drop using assumed power, power distribution, inlet and outlet temperature, the system pressure, fuel size and fuel type as input data.

The options for fuel type are of the pebble type; the multi holes block type and the pin-in-block type. The power distribution for cases of cosine and exponential is available., The users can calculate for the other distributions by preparing the input file.

The maximum fuel temperature will be calculated in PEPTEMP as follows:

$$T_{max}(z) = T_{in} + \Delta T_{cl}(z) + \Delta T_{film}(z) + \Delta T_{sl}(z) + \Delta T_{com} \quad (1)$$

where $T_{max}(z)$: fuel temperature at the center of fuel element i.e. the maximum fuel temperature; ΔT_{cl} : gas temperature increment from inlet to height z ; T_{in} : gas inlet temperature; $\Delta T_{film}(z)$: temperature difference between fuel element surface and coolant gas at z ; $\Delta T_{sl}(z)$: temperature difference between

fuel matrix outer surface and fuel element surface; $\Delta T_{com}(z)$: temperature difference between fuel matrix outer surface and fuel center; q''' : power density; A_j : fuel element surface area; z : axial distance from the top of the core; C_p : coolant heat capacity.

3.2. Temperature Difference in the Spherical Fuel Element

Figure 4 shows fuel configuration of the solid type and the shell type fuel element. In the solid type, ΔT_{com} is given as follows

$$\Delta T_{com}(z) = T_{co} - T_c = \frac{q'''(z)r_c^2}{6\lambda_c} \quad (2)$$

In the case of the shell type fuel element, ΔT_{com} can be calculated by the following expression;

$$\Delta T_{com}(z) = T_{co} - T_c = \frac{q'''(z)}{6\lambda_c} \left(r_c^2 - 3r_{co}^2 + \frac{2r_{co}^3}{r_c} \right) \quad (3)$$

3.3. Film Temperature Difference

The film temperature differences are calculated as follows;

$$\Delta T_{film} = T_s - T_{ch} = \frac{q'''(z)r_c^3}{3r_s^2h} \quad (4)$$

3.4. Heat Transfer Coefficient

Heat transfer coefficient h in Equation (4) is calculated using the following correlation [10]:

$$h = 0.68\rho v_s C_p Re^{-0.3} Pr^{-0.66} \quad (5)$$

$$Re = \frac{\rho v_s d}{(1-\varepsilon)\mu} \quad (6)$$

where, ρ : coolant density; v_s : coolant velocity; Re: Reynolds number; Pr: Prandtl number; ε : Porosity; d : fuel element diameter and μ : viscosity of fluid.

Reactor structure of UHTREX

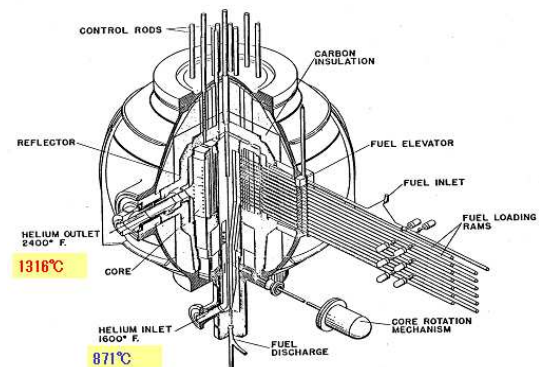


Fig. 1. Reactor structure of UHTREX, quoted from reference [3].

Table 1. Major nuclear and thermal-hydraulic specification.

Thermal power (MW)	300 / 450 / 600
Coolant	Helium
Inlet coolant temperature (oC)	550
Outlet coolant temperature (oC)	900 (900 – 1650 oC)
Coolant Pressure (MPa)	6.0 (1 – 15 MPa)
Total coolant flow rate (kg/s)	172.1 / 258.2 / 344.2
Core coolant flow rate (kg/s)	165.2 / 247.8 / 320.8
Core diameter (m)	2.91
Core height (m)	9.4
Core fuel porosity (–)	0.39 (0.26 – 0.50)
Average power density (MW/m ³)	4.8 / 7.2 / 9.6
Fuel type (for standard case)	6 cm diameter pebble

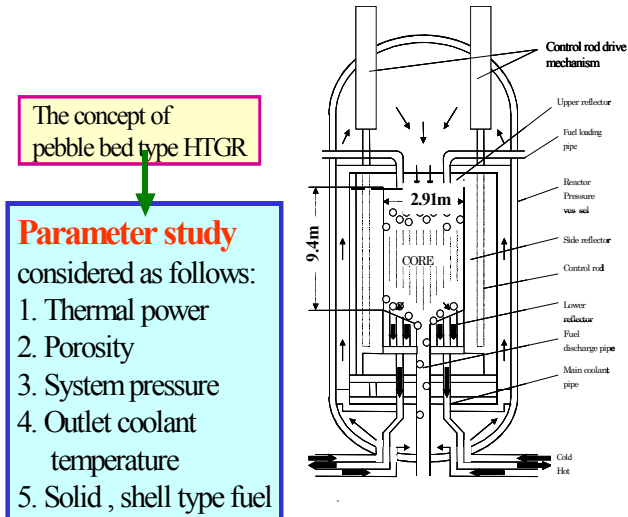
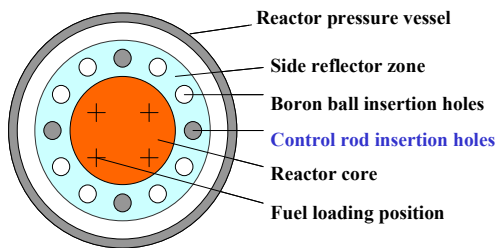


Fig. 2. A concept of pebble bed reactor of HTGR –GT300.

Figure Core arrangement plane view



Four percent Coolant flows Control rod insertion holes.
 W_{eff} : effective coolant flow rate that has dimensionless value due to the normalization by the total coolant flow rate.
 Maximum W_{eff} is 0.96.

Fig. 3. Core arrangement plane view.

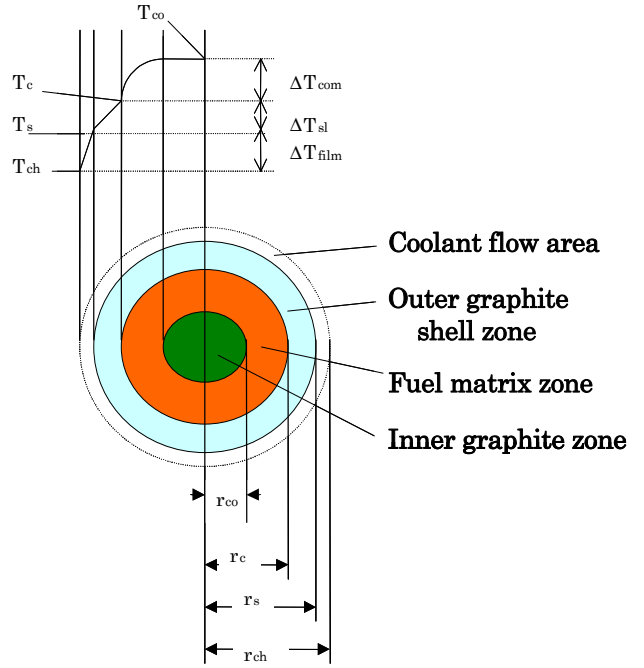


Fig. 4. Relation of shell type fuel element and temperature difference, in the case that no inner graphite zone is called the solid type, i.e., $r_{co}=0$.

Analysis method

Fuel Temperature analysis code for High Temperature gas-cooled reactor
PEBTEMP

The option of thermal power distribution are as follows:

- (1) Cosine
- (2) exponential i.e. same fuel center temperature in axial

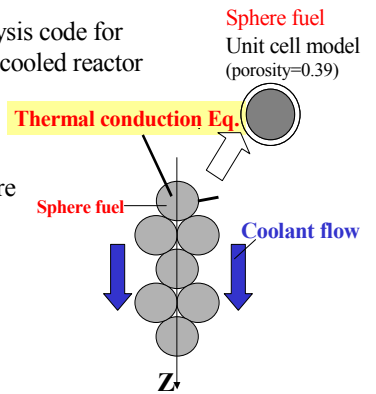


Fig. 5. Analysis method of thermal-hydraulic computer code PEBTEMP.

Parameter	Fuel element type		
	Hollow-rod	Multi-hole	Pebble-bed
Heat transfer area of fuel (m ²)	777	1073	3814
Heat transfer coefficient (W/m ² K)	2101	2801	4037

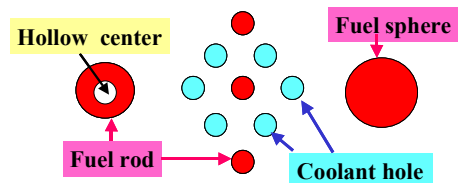


Fig. 6. Heat transfer performances in the small size reactor design by handy evaluation.

Table 2. Analysis cases and fuel maximum temperature in the 300MW of thermal power i.e.GT300.

Case	P(MPa)	Tout	$\epsilon=0.26$	$\epsilon=0.39$	$\epsilon=0.40$	$\epsilon=0.50$
A01	1	900	983.7	1015.6	1019	1060.3
A02	1	1150	1209	1236.4	1239	1274.3
A03	1	1400	1446.7	1468.9	1471	1502
A04	1	1650	1688.9	1707.4	1709.6	1736.6
A05	5	900	983.7	1015.6	1019	1060.2
A06	5	1150	1209	1236.4	1239	1274.2
A07	5	1400	1446.7	1468.8	1471	1501.9
A08	5	1650	1688.8	1707.4	1709.6	1736.6
A09	6	900	983.7	1015.6	1019	1053.8
A10	6	1150	1209	1236.3	1239	1274.2
A11	6	1400	1446.7	1468.8	1471	1501.9
A12	6	1650	1688.8	1707.4	1709.6	1736.6
A13	10	900	983.7	1015.6	1019	1060.2
A14	10	1150	1209	1236.3	1238.9	1274.2
A15	10	1400	1446.7	1468.8	1470.9	1501.9
A16	10	1650	1688.8	1707.4	1709.6	1736.6
A17	15	900	983.7	1015.6	1019	1060.1
A18	15	1150	1208.9	1236.3	1238.9	1274.2
A19	15	1400	1446.7	1468.8	1470.9	1501.9
A20	15	1650	1688.8	1707.4	1709.6	1736.6

3.5. Pressure Drop

Pressure drop through the core expresses by the following correlation [6]:

$$\Delta P = 6.986 \frac{(1-\epsilon)^{n+1}}{\epsilon^3} \text{Re}_p^{-n} \rho v_s^2 \frac{H}{d} K + \Delta P_a \tag{7}$$

$$n=0.22 \tag{8}$$

$$K = 1 - 0.26(1+n+3 \frac{1-\epsilon}{\epsilon}) \frac{d}{R} \tag{9}$$

$$\text{Re}_p = \frac{\rho v_s d}{\eta} \tag{10}$$

where, H : core height; R : core radius and ΔP_a : acceleration pressure drop.

3.6. Effective Flow Rate Consideration

As many blocks of graphite form the reflector, there exist gaps by which the coolant flow may pass through [11]. Actually, only one portion of coolant passes through the reactor core from the top to the bottom. This portion is called effective flow rate and can be calculated iteratively in the code. The empirical equation used in this code is as follows [11]:

$$W_{eff} = 0.98 - 0.012\Delta P \tag{11}$$

where, W_{eff} : effective coolant flow rate that has dimensionless value due to the normalization by the total coolant flow rate.

ΔP : pressure drop through the core

4. Calculation Results

4.1. Handy Calculation Results for Small Scale HTGR

Before the main calculation, we have done the prediction study of the comparison of key factors of heat transfer in the small scale HTGR with three types of different fuel elements. They are the hollow-rod [3], the multi-hole [1,8] and the pebble-bed [10]. The small reactor thermal data are as follows; thermal power of 50MW, power density of 2.5 MW/m³ and inlet/ outlet coolant temperature of 395 °C/ 850 °C, respectively. Figure 6 shows the results of heat transfer area in the core and heat transfer coefficient on the fuel surface. Heat transfer area of the pebble-bed is 5 times larger than that of the hollow-rod. Heat transfer coefficient of the pebble-bed is twice larger than that of the hollow-rod. Therefore heat transfer performance of pebble-bed is superior to other types of fuel elements.

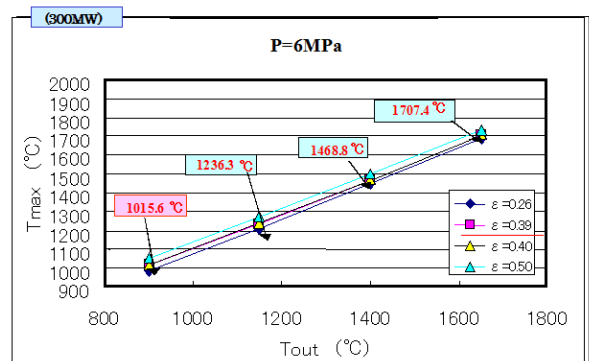


Fig. 7. Dependence of maximum fuel temperature on outlet coolant temperature for GT300 with different porosity and $W_{eff}=1$.

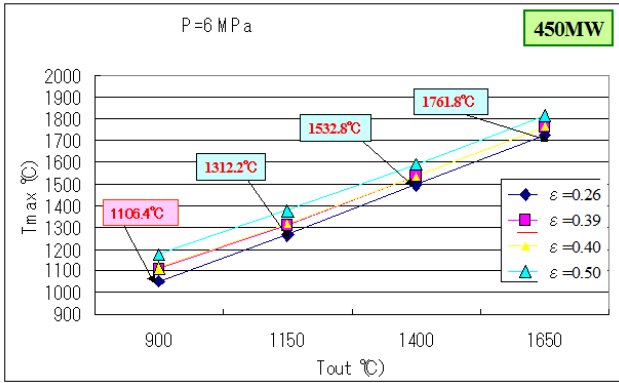


Fig. 8. Dependence of maximum fuel temperature on outlet coolant temperature for GT450 with different porosity and $W_{eff}=1$.

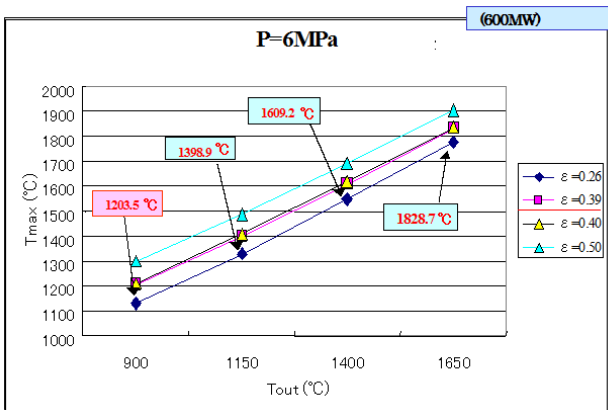


Fig. 9. Dependence of maximum fuel temperature on outlet coolant temperature for GT600 with different porosity and $W_{eff}=1$.

4.2. Temperature Calculation for HTGR-GT300 to GT600

Table 2 shows the 20 analysis cases and fuel maximum temperature in the 300MW of thermal power i.e.GT300. The system pressure ranges from 1 MPa through 15 MPa. The system pressure does not have any effect on the fuel maximum temperature. Thus we focus our intension to 6 MPa of system pressure [1]. Figure 7, 8 and 9 show the dependence of maximum fuel temperature on outlet coolant temperature for GT300, GT450 and GT-600 with different porosity and $W_{eff}=1$. The maximum fuel temperature for GT600 is 168 °C higher than that for GT300 where the outlet coolant temperature is 900 °C and the porosity is 0.39. The maximum fuel temperature for GT-600 is 163 °C higher than that for GT-300, where the outlet coolant temperature is 1150 °C and the porosity is 0.39. The high porosity leads to low fuel maximum temperature.

4.3. Pressure Drop Calculation for HTGR-GT300 to GT600

Table 3 shows the 20 analysis cases and pressure drop (ΔP) in the core of 300MW of thermal power. The system pressure ranges from 1 MPa through 15 MPa. The high system pressure

leads to low-pressure drop in the core. In the case of 6 MPa of system pressure, the ΔP changes from 40.2 kPa to 16.7 kPa, where the T_{out} increases from 900 °C to 1150 °C. The ΔP changes from 16.7 kPa to 6.3 kPa, where the porosity increases from 0.39 to 0.50 with 1150 °C of T_{out} . The high porosity leads to low-pressure drop. In the case of 15 MPa of system pressure, the ΔP changes from 16.7 kPa to 6.7 kPa, where the T_{out} increases from 900 °C to 1150 °C. The ΔP changes from 6.7 kPa to 2.6 kPa, where the porosity increases from 0.39 to 0.50 with 1150 °C of T_{out} .

Table 4 shows the 20 analysis cases and pressure drop (ΔP) in the core of 450MW of thermal power. The system pressure ranges from 1 MPa through 15 MPa. The high system pressure leads to low-pressure drop in the core. In the case of 6 MPa of system pressure, the ΔP changes from 86.2 kPa to 35.3 kPa, where the T_{out} increases from 900 °C to 1150 °C. The ΔP changes from 35.3 kPa to 13.7 kPa, where the porosity increases from 0.39 to 0.50 with 1150 °C of T_{out} . The high porosity leads to low-pressure drop. In the case of 15 MPa of system pressure, the ΔP changes from 35.3 kPa to 14.7 kPa, where the T_{out} increases from 900 °C to 1150 °C. The ΔP changes from 14.7 kPa to 5.5 kPa, where the porosity increases from 0.39 to 0.50 with 1150 °C of T_{out} .

Table 5 shows the 20 analysis cases and pressure drop (ΔP) in the core of 600MW of thermal power. The system pressure ranges from 1 MPa through 15 MPa. The high system pressure leads to low-pressure drop in the core. In the case of 6 MPa of system pressure, the ΔP changes from 147 kPa to 60.8 kPa, where the T_{out} increases from 900 °C to 1150 °C. The ΔP changes from 60.8 kPa to 23.5 kPa, where the porosity increases from 0.39 to 0.50 with 1150 °C of T_{out} . The high porosity leads to low-pressure drop. In the case of 15 MPa of system pressure, the ΔP changes from 59.8 kPa to 24.5 kPa, where the T_{out} increases from 900 °C to 1150 °C. The ΔP changes from 24.5 kPa to 9.4 kPa, where the porosity increases from 0.39 to 0.50 with 1150 °C of T_{out} .

Available pressure drop evaluation

$W_{eff} \geq 0.70$
 From eq.(11)
 $\Delta P \leq 23.3 \text{ kPa}$

How to decrease pressure drop

- High system pressure
- High porosity
- Large sphere fuel diameter

Fig. 10. The procedures to evaluate the pressure drop considering the available effective coolant flow rate.

Table 3. Analysis cases and pressure drop in the GT300.

Case	P(MPa)	Tout	$\epsilon = 0.26$	$\epsilon = 0.39$	$\epsilon = 0.40$	$\epsilon = 0.50$
A01	1	900	9.80E+02	2.35E+02	2.16E+02	9.11E+01
A02	1	1150	4.12E+02	9.80E+01	8.92E+01	3.72E+01
A03	1	1400	2.35E+02	5.78E+01	5.19E+01	2.16E+01
A04	1	1650	1.67E+02	3.92E+01	3.63E+01	1.47E+01
A05	5	900	1.96E+02	4.80E+01	4.41E+01	1.86E+01
A06	5	1150	8.23E+01	1.96E+01	1.76E+01	7.55E+00
A07	5	1400	4.80E+01	1.18E+01	1.08E+01	4.41E+00
A08	5	1650	2.74E+01	7.94E+00	7.15E+00	3.04E+00
A09	6	900	1.67E+02	4.02E+01	3.63E+01	1.57E+01
A10	6	1150	6.86E+01	1.67E+01	1.47E+01	6.27E+00
A11	6	1400	4.02E+01	9.60E+00	8.72E+00	3.72E+00
A12	6	1650	2.74E+01	6.57E+00	5.98E+00	2.55E+00
A13	10	900	9.80E+01	2.45E+01	2.16E+01	9.21E+00
A14	10	1150	4.12E+01	9.80E+00	9.02E+00	3.82E+00
A15	10	1400	2.45E+01	5.78E+00	5.29E+00	2.25E+00
A16	10	1650	1.67E+01	3.92E+00	3.63E+00	1.57E+00
A17	15	900	6.76E+01	1.67E+01	1.47E+01	6.17E+00
A18	15	1150	2.74E+01	6.66E+00	6.08E+00	2.55E+00
A19	15	1400	1.57E+01	3.82E+00	3.53E+00	1.47E+00
A20	15	1650	1.08E+01	2.65E+00	2.45E+00	9.80E-01

Table 4. Analysis cases and pressure drop in the GT450.

Case	P(MPa)	Tout	$\epsilon = 0.26$	$\epsilon = 0.39$	$\epsilon = 0.40$	$\epsilon = 0.50$
A01	1	900	2.16E+03	5.19E+02	4.70E+02	1.96E+02
A02	1	1150	8.82E+02	2.16E+02	1.96E+02	8.13E+01
A03	1	1400	5.10E+02	1.27E+02	1.08E+02	4.70E+01
A04	1	1650	3.53E+02	8.43E+01	7.64E+01	3.23E+01
A05	5	900	4.31E+02	1.08E+02	9.41E+01	3.92E+01
A06	5	1150	1.76E+02	6.32E+03	3.82E+01	1.67E+01
A07	5	1400	1.08E+02	2.45E+01	2.25E+01	9.51E+00
A08	5	1650	5.88E+01	1.67E+01	1.57E+01	6.47E+00
A09	6	900	3.63E+02	8.62E+01	7.84E+01	3.33E+01
A10	6	1150	1.47E+02	3.53E+01	3.23E+01	1.37E+01
A11	6	1400	8.62E+01	2.06E+01	1.86E+01	7.94E+00
A12	6	1650	5.88E+01	1.37E+01	1.27E+01	5.39E+00
A13	10	900	2.16E+02	5.19E+01	4.70E+01	1.96E+01
A14	10	1150	8.92E+01	2.16E+01	1.96E+01	8.13E+00
A15	10	1400	5.19E+01	1.27E+01	1.18E+01	4.70E+00
A16	10	1650	3.53E+01	8.53E+00	7.74E+00	3.23E+00
A17	15	900	1.47E+02	3.53E+01	3.14E+01	1.37E+01
A18	15	1150	5.98E+01	1.47E+01	1.27E+01	5.49E+00
A19	15	1400	3.43E+01	8.33E+00	7.55E+00	3.14E+00
A20	15	1650	2.35E+01	5.68E+00	5.19E+00	2.16E+00

Table 5. Analysis cases and pressure drop in the GT600.

Case	P(MPa)	Tout	$\epsilon = 0.26$	$\epsilon = 0.39$	$\epsilon = 0.40$	$\epsilon = 0.50$
A01	1	900	3.72E+03	8.92E+02	8.13E+02	3.43E+02
A02	1	1150	1.57E+03	3.63E+02	3.33E+02	1.37E+02
A03	1	1400	8.82E+02	2.16E+02	1.96E+02	8.13E+01
A04	1	1650	6.08E+02	1.47E+02	1.27E+02	5.59E+01
A05	5	900	7.45E+02	1.76E+02	1.67E+02	6.86E+01
A06	5	1150	3.04E+02	7.35E+01	6.66E+01	2.84E+01
A07	5	1400	1.76E+02	4.21E+01	3.92E+01	1.67E+01
A08	5	1650	9.80E+01	2.94E+01	2.65E+01	1.08E+01
A09	6	900	6.17E+02	1.47E+02	1.37E+02	5.68E+01
A10	6	1150	2.55E+02	6.08E+01	5.59E+01	2.35E+01
A11	6	1400	1.47E+02	3.53E+01	3.23E+01	1.37E+01
A12	6	1650	9.80E+01	2.45E+01	2.25E+01	9.31E+00
A13	10	900	3.72E+02	9.02E+01	8.13E+01	3.43E+01
A14	10	1150	1.57E+02	3.72E+01	3.33E+01	1.37E+01
A15	10	1400	8.92E+01	2.16E+01	1.96E+01	8.13E+00
A16	10	1650	6.08E+01	1.47E+01	1.37E+01	5.59E+00
A17	15	900	2.55E+02	5.98E+01	5.49E+01	2.25E+01
A18	15	1150	9.80E+01	2.45E+01	2.25E+01	9.41E+00
A19	15	1400	5.98E+01	1.47E+01	1.27E+01	5.49E+00
A20	15	1650	4.12E+01	9.80E+00	8.92E+00	3.72E+00

Table 6. The available analysis cases in the GT300 considering the design limits.

Case	P(MPa)	Tout	$\epsilon=0.26$	$\epsilon=0.39$	$\epsilon=0.40$	$\epsilon=0.50$
A01	1	900	983.7	1016	1019	1060
A02	1	1150	1209	1236	1239	1274
A05	5	900	983.7	1015.6	1019	1060.2
A06	5	1150	1209	1236.4	1239	1274.2
A09	6	900	983.7	1016	1019	1054
A10	6	1150	1209	1236	1239	1274
A13	10	900	983.7	1015.6	1019	1060.2
A14	10	1150	1209	1236.3	1238.9	1274.2
A17	15	900	983.7	1016	1019	1060
A18	15	1150	1208.9	1236	1239	1274

Case	P(MPa)	Tout	$\epsilon=0.26$	$\epsilon=0.39$	$\epsilon=0.40$	$\epsilon=0.50$
A03	1	1400				2.16E+01
A04	1	1650				1.47E+01
A05	5	900				1.86E+01
A06	5	1150		1.96E+01	1.76E+01	7.55E+00
A09	6	900				1.57E+01
A10	6	1150		1.67E+01	1.47E+01	6.27E+00
A13	10	900			2.16E+01	9.21E+00
A14	10	1150		9.80E+00	9.02E+00	3.82E+00
A17	15	900		1.67E+01	1.47E+01	6.17E+00
A18	15	1150		6.66E+00	6.08E+00	2.55E+00

Design Limit of maximum fuel temperature(°C) and pressure drop (kPa) in 300MW thermal power

Design Limit

Tmax \cong 1300°C

Δ Pmax \cong 23.3kPa

Table 7. The available analysis cases in the GT600 considering the design limits.

Case	P(MPa)	Tout	$\epsilon=0.26$	$\epsilon=0.39$	$\epsilon=0.40$	$\epsilon=0.50$
A01	1	900	1130.3	1203.5	1210.5	1297.9
A05	5	900	1130.3	1203.5	1210.5	1297.9
A09	6	900	1130.3	1203.5	1210.4	1297.9
A13	10	900	1130.3	1203.4	1210.4	1297.8
A17	15	900	1130.3	1203.4	1210.4	1297.8

Case	P(MPa)	Tout	$\epsilon=0.26$	$\epsilon=0.39$	$\epsilon=0.40$	$\epsilon=0.50$
A07	5	1400				1.67E+01
A08	5	1650				1.08E+01
A10	6	1150				2.35E+01
A11	6	1400				1.37E+01
A12	6	1650			2.25E+01	9.31E+00
A14	10	1150				1.37E+01
A15	10	1400		2.16E+01	1.96E+01	8.13E+00
A16	10	1650		1.47E+01	1.37E+01	5.59E+00
A17	15	900				2.25E+01
A18	15	1150			2.25E+01	9.41E+00
A19	15	1400		1.47E+01	1.27E+01	5.49E+00
A20	15	1650		9.80E+00	8.92E+00	3.72E+00

Design Limit of maximum fuel temperature(°C) and pressure drop (kPa) in 600MW thermal power

Design Limit:

Tmax \cong 1300°C

Δ Pmax \cong 23.3kPa

4.4. Consideration of Available Reactor Core Design

The traditional design limits in Japan suggested that the maximum fuel temperature should be lower than 1300 °C. From the engineering judgments, the effective coolant flow rate should be higher than 70 %. Thus the design limit of the

pressure drop in the core is 23.3 kPa, according to the eq. (11) as shown in Figure 10. Table 6 and 7 show the available analysis cases of GT300 and GT600. The available analysis cases in GT300 are case A05, A06, A09, A10, A13, A14, A17, and A18. It means that 1150 °C of the outlet coolant temperature is available. On the contrary, the available

analysis case in GT600 is the case A17. It means that 900 °C of the outlet coolant temperature is available.

5. Conclusions

The followings can be concluded:

1. High porosity leads to low fuel maximum temperature.
2. High system pressure leads to low-pressure drop in the core.
3. High porosity leads to low-pressure drop.
4. The available analysis cases in 300MW of thermal power are 8 cases, which indicates that the outlet coolant temperature is lower than 1150 °C.
5. On the contrary, the available analysis case in 600MW of thermal power is only 1 case, which indicate that the outlet coolant temperature is up to 900 °C.

Nomenclature

A_f : fuel element surface area; (m²)
 C_p : coolant heat capacity; (J/kgK)
 H : core height; (m)
 h : heat transfer coefficient; (W/m²K)
 q''' : power density; (W/m³)
 R : core radius; (m)
 Re : Reynolds number
 $T_f(z)$: fuel temperature at the center of fuel element, i.e., the maximum fuel temperature; (°C)
 T_{in} : gas inlet temperature; (°C)
 T_{out} : gas outlet temperature; (°C)
 W_{eff} : effective coolant flow rate, dimensionless value due to the normalization
 z : axial distance from the top of the core; (m)
 ΔP : pressure drop through the core (kPa)
 ΔP_a : acceleration pressure drop; ((kPa)
 ΔT_{ci} : gas temperature increment from inlet to height z ; (°C)
 $\Delta T_{com}(z)$: temperature difference between fuel matrix outer surface and fuel center; (°C)

$\Delta T_{film}(z)$: temperature difference between fuel element surface and coolant gas at z ; (°C)

$\Delta T_{sl}(z)$: temperature difference between fuel matrix outer surface and fuel element surface; (°C)

References

- [1] A Technology Roadmap for Generation IV Nuclear Energy Systems, GIF-002-00, Generation IV International Forum (2002), <http://gif.inel.gov/roadmap/>
- [2] Shusaku SHIOZAWA et al., "The HTTR Project as the World Leader of HTGR Research and Development", J. of AESJ Vol.47, pp. 342-349 (2005)
- [3] B.M. HOGLUND, "UHTREX Operation Near", Vol.9, pp. 1, Power Reactor Technology (1966)
- [4] "UHTREX: Alive and Running with Coolant at 2400 oF", Nuclear News (1969)
- [5] Progress Report – Pebble Bed Reactor Program, NYO-9071, US Atomic Energy Commission (1960)
- [6] M.M.El-Wakil, Nuclear Energy Conversion, Thomas Y. Crowell Company Inc., USA (1982)
- [7] M.M El-Wakil, Nuclear Heat Transport, International Textbook Company, USA (1971)
- [8] Motoo Fumizawa et al., "Effective Coolant Flow Rate of Flange Type Fuel Element for Very High Temperature Gas-Cooled Reactor ", J. of AESJ Vol.31, pp 828-836 (1989)
- [9] Motoo Fumizawa et al., "Preliminary Study for Analysis of Gas-cooled Reactor with Sphere Fuel Element ", AESJ Spring MTG, I66 (2000)
- [10] Fumizawa, M.; Nuclear Reactors (ISBN 978-953-51-0967 -9), Edited by Amir Zacarias Mesquita, InTech, pp.177-191 (2013)
- [11] Motoo Fumizawa et al., "The Conceptual Design of High Temperature Engineering Test Reactor Upgraded through Utilizing Pebble-in-block Fuel", JAERI-M 89-222 (1989)